

Research Article: New Research | Disorders of the Nervous System

Post-Stroke Intranasal (+)-Naloxone Delivery Reduces Microglial Activation and Improves Behavioral Recovery from Ischemic Injury

Jenni E. Anttila¹, Katrina Albert¹, Emily S. Wires², Kert Mätlik^{1,3}, Lisa Loram⁴, Linda Watkins⁴, Kenner C. Rice², Yun Wang^{2,5}, Brandon K. Harvey² and Mikko Airavaara^{1,2}

¹Institute of Biotechnology, HiLIFE Unit, University of Helsinki, 00014, Finland P.O. Box 56

²Intramural Research Program, National Institute on Drug Abuse, IRP, NIH, Baltimore, MD 21224, USA

³Medicum, Department of Pharmacology, University of Helsinki, 00014, Finland

⁴Department of Psychology & Neuroscience, University of Colorado, Boulder, CO 80309, USA

⁵Center for Neuropsychiatric Research, National Health Research Institutes, Zhunan, 35053, Taiwan

DOI: 10.1523/ENEURO.0395-17.2018

Received: 17 November 2017

Revised: 12 March 2018

Accepted: 20 March 2018

Published: 16 April 2018

Author contributions: JEA, BKH & MA: conception and design; JEA, KA, ESW, KM, LL, LW, KR, YW, BKH and MA collection and assembly of data, data analysis and interpretation, manuscript writing; BKH & MA financial support and final approval of manuscript.

Funding: <http://doi.org/10.13039/501100005878>–Academy of Finland | Terveystieteiden tutkimuskeskuksen Toimikunta (Forskningsrådet för Hälsa): 250275; #256398; #281394. Biocentrum Helsinki; <http://doi.org/10.13039/501100006306>–Sigrid Juséliuksen Säätiö (Sigrid Jusélius Stiftelse); EU FP7: GLORIA ID: 602919. <http://doi.org/10.13039/501100003406>–Tekes (Finnish Funding Agency for Innovation): 3iRegeneration. National Institute on Drug Abuse, Intramural research program, NIH, USA; <http://doi.org/10.13039/501100003502>–Ella ja Georg Ehrnroothin Säätiö (Ella and Georg Ehrnrooth Foundation); Päivikki and Sakari Sohlberg Foundation; <http://doi.org/10.13039/100008969>–Alfred Kordelinin Säätiö (Alfred Kordelin Foundation); <http://doi.org/10.13039/5011000070830>–Orionin Tutkimussäätiö (Orion Research Foundation);

Conflict of Interest: Authors report no conflict of interest.

This work was supported by Academy of Finland grants: #250275, #256398, #281394; Biocentrum Helsinki; Sigrid Jusélius Foundation; EU FP7 GLORIA ID: 602919, 3iRegeneration funded by Tekes, and the National Institute on Drug Abuse, Intramural Research Program at the National Institutes of Health. KCR was also supported by the National Institute on Alcohol Abuse and Alcoholism. JEA was also funded by Ella and Georg Ehrnrooth Foundation, Päivikki and Sakari Sohlberg Foundation, Alfred Kordelin Foundation and Orion Research Foundation.

B.K.H. and M.A. have equal contribution for the senior corresponding author position.

Correspondence should be addressed to either Brandon K. Harvey, PhD, National Institute on Drug Abuse, Intramural research program, National Institutes of Health, 251 Bayview Blvd, Baltimore, MD 21224, USA. Phone: 443 740 2592, E-mail: bharvey@intra.nida.nih.gov or Mikko Airavaara, PhD, Institute of Biotechnology, P.O. Box 56 (Viikinkaari 5D), 00014 University of Helsinki, Finland. Cell: + 358405112175, E-mail: mikko.airavaara@helsinki.fi

Cite as: eNeuro 2018; 10.1523/ENEURO.0395-17.2018

Alerts: Sign up at eneuro.org/alerts to receive customized email alerts when the fully formatted version of this article is published.

Accepted manuscripts are peer-reviewed but have not been through the copyediting, formatting, or proofreading process.

Copyright © 2018 Anttila et al.

This is an open-access article distributed under the terms of the Creative Commons Attribution 4.0 International license, which permits unrestricted use, distribution and reproduction in any medium provided that the original work is properly attributed.

1 **Manuscript title: Post-stroke intranasal (+)-naloxone delivery reduces microglial activation**
2 **and improves behavioral recovery from ischemic injury**

3

4 **Abbreviated title: Post-stroke (+)-naloxone promotes recovery**

5

6 **Authors:** Jenni E. Anttila¹, Katrina Albert¹, Emily S. Wires², Kert Mätlik^{1, 3}, Lisa Loram⁴,
7 Linda Watkins⁴, Kenner C. Rice², Yun Wang^{2,5}, Brandon K. Harvey^{*2}, Mikko Airavaara^{*1,2}

8

9 **Affiliations:**

10 ¹ Institute of Biotechnology, HiLIFE unit, P.O. Box 56, 00014 University of Helsinki, Finland.

11 ² Intramural Research Program, National Institute on Drug Abuse, IRP, NIH, Baltimore, MD
12 21224, USA.

13 ³ Medicum, Department of Pharmacology, 00014 University of Helsinki, Finland

14 ⁴ Department of Psychology & Neuroscience, University of Colorado, Boulder, CO 80309, USA.

15 ⁵ Center for Neuropsychiatric Research, National Health Research Institutes, Zhunan 35053,
16 Taiwan.

17

18 * The authors have equal contribution for the senior corresponding author position

19

20 **Author contributions:** JEA, BKH & MA: conception and design; JEA, KA, ESW, KM, LL,
21 LW, KR, YW, BKH and MA collection and assembly of data, data analysis and interpretation,
22 manuscript writing; BKH & MA financial support and final approval of manuscript.

23

24 **Correspondence should be addressed to:**

25 Brandon K. Harvey Ph.D.

26 National Institute on Drug Abuse

27 Intramural research program

28 National Institutes of Health
29 251 Bayview Blvd
30 Baltimore, MD 21224, USA
31 Phone: 443 740 2592
32 Email: bharvey@intra.nida.nih.gov

33
34 Mikko Airavaara Ph.D.
35 Institute of Biotechnology
36 P.O. Box 56 (Viikinkaari 5D)
37 00014 University of Helsinki, Finland
38 Cell: + 358405112175
39 Email: mikko.airavaara@helsinki.fi

40

41 Number of figures: 9	45 Number of words for Significance
42 Number of tables: 1	46 statement: 118
43 Number of multimedia: 0	47 Number of words for Introduction: 663
44 Number of words for Abstract: 219	48 Number of words for Discussion: 1615

49

50 **Acknowledgements:** Congjun Zheng, Paula Collin-Olkkonen and Suvi Pöyhönen are
51 acknowledged for technical assistance.

52

53 **Conflict of Interest:** The authors declare no competing financial interests.

54

55 **Funding sources:** This work was supported by Academy of Finland grants: #250275, #256398,
56 #281394; Biocentrum Helsinki; Sigrid Jusélius Foundation; EU FP7 GLORIA ID: 602919,
57 3iRegeneration funded by Tekes, and the National Institute on Drug Abuse, Intramural Research
58 Program at the National Institutes of Health. KCR was also supported by the National Institute
59 on Alcohol Abuse and Alcoholism. JEA was also funded by Ella and Georg Ehrnrooth
60 Foundation, Päivikki and Sakari Sohlberg Foundation, Alfred Kordelin Foundation and Orion

61 Research

Foundation.

62 **Abstract**

63 Ischemic stroke is the leading cause of disability, and effective therapeutic strategies are needed
64 to promote incomplete recovery. Neuroinflammation plays a significant role in stroke
65 pathophysiology, and there is limited understanding how it affects recovery. The aim of the study
66 was to characterize the spatiotemporal expression profile of microglial activation and to study
67 whether dampening microglial/macrophage activation post-stroke facilitates the recovery. For
68 dampening microglial/macrophage activation we chose intranasal administration of naloxone, a
69 drug that is already in clinical use for opioid overdose and is known to decrease
70 microglia/macrophage activation. We characterized the temporal progression of
71 microglia/macrophage activation following cortical ischemic injury in rat and found the peak
72 activation in cortex 7 days post-stroke. Unexpectedly, there was a chronic expression of
73 phagocytic cells in the thalamus associated with neuronal loss. (+)-Naloxone, an enantiomer that
74 reduces microglial activation without antagonizing opioid receptors, was administered
75 intranasally starting 1 day post-stroke and continuing for 7 days. (+)-Naloxone treatment
76 decreased microglia/macrophage activation in the striatum and thalamus, promoted behavioral
77 recovery during the 14-day monitoring period, and reduced neuronal death in the lesioned cortex
78 and ipsilateral thalamus. Our results are the first to show that post-stroke intranasal (+)-naloxone
79 administration promotes short-term functional recovery and reduces microglia/macrophage
80 activation. Therefore, (+)-naloxone is a promising drug for the treatment of ischemic stroke and
81 further studies should be conducted.

82

83 **Significance statement**

84 Ischemic stroke is one of the leading causes of adult disability and new drug treatments are
85 needed as there is no drug that would promote the recovery. Neuroinflammation is suggested to
86 play a role in the recovery process. Naloxone is a drug used clinically to treat opioid overdose.
87 Its opioid receptor inactive form, (+)-naloxone, is known to reduce the activation of microglia,
88 the immune cells of the brain. We show for the first time that repeated dosing of intranasal (+)-
89 naloxone starting one day after stroke promotes short-term recovery in rats, reduces microglial
90 activation and neuronal loss in the stroke brain. Our finding could be important for future stroke
91 treatment and encourages further testing of (+)-naloxone in stroke patients.

92

93 **Introduction**

94 Approximately 10 million patients survive a stroke each year, however there are currently no
95 pharmacological options to promote recovery. Neurological deficits including impaired use of
96 contralateral limbs, sensory and cognitive deficits and problems in speaking are the primary
97 cause of disability and remain without effective treatment. Despite increased knowledge of the
98 cellular and molecular mechanisms that mediate damage and recovery after stroke, the
99 development of new drugs for stroke has been unsuccessful (Dirnagl, 2012). Most studies have
100 focused on neuroprotection, and therefore, there is a great need to find novel drug targets, and
101 develop new treatments that would improve the recovery from ischemic brain injury by targeting
102 the post-ischemic pathological mechanisms such as inflammation. Modulation of brain
103 inflammatory cascades following stroke is recognized as a viable therapeutic strategy to promote
104 functional recovery from ischemic brain injury (Endres et al., 2008). However, very few studies
105 have taken this approach, and little is known about recovery from stroke in relation to
106 neuroinflammation.

107

108 The drug naloxone, an opiate antagonist, has been clinically used for opioid overdose for nearly
109 50 years, has anti-inflammatory properties and can attenuate microglial activation. Naloxone has
110 two stereoisomers, the (-) and (+) enantiomers (Fig. 1). (-)-Naloxone has a high affinity for
111 antagonizing μ , δ , and κ opioid receptors, whereas (+)-naloxone, has a very low affinity for
112 opioid receptors (Iijima et al., 1978). Clinical reports indicate that intravenously administered (-
113)-naloxone ameliorates neurological deficits in acute stroke (Baskin and Hosobuchi, 1981;
114 Jabaily and Davis, 1984). Studies examining the neuroprotective effect of (-)-naloxone in rat
115 focal cerebral ischemia also showed a significant reduction in neuronal loss and inflammation

116 (Chen et al., 2001; Liao et al., 2003), but (+)-naloxone did not affect the infarction volume when
117 administered before ischemia. These differences between (-) and (+) isoforms suggest a role for
118 opioid receptor antagonism in the neuroprotective effect (Liao et al., 2003). However, both
119 enantiomers have been shown to reduce the number of activated microglia in a rat model of
120 neuropathic pain (Hutchinson et al., 2008), and to inhibit superoxide production from microglia,
121 and subsequent neurodegeneration, by interacting with NADPH oxidase (Liu et al., 2002; Qin et
122 al., 2005; Wang et al., 2012). Also, both naloxone enantiomers reduce lipopolysaccharide (LPS)-
123 induced microglial activation and protect neurons from LPS-induced neurodegeneration (Liu et
124 al., 2000a; Liu et al., 2000b; Liu et al., 2000c). LPS signaling in microglia/macrophages requires
125 Toll-like receptor 4 (TLR4) that is expressed abundantly on microglia (Lehnardt et al., 2003).
126 Both (-)- and (+)-naloxone enantiomers decrease LPS-induced TLR4 signaling (Hutchinson et
127 al., 2008; Wang et al., 2016) and both have been shown to antagonize the TLR4 coreceptor MD2
128 (Hutchinson et al., 2012). TLR4 activation leads to activation of NF- κ B, and production of pro-
129 inflammatory cytokines, interferons, and reactive oxygen/nitrogen species. TLR4 deficiency is
130 neuroprotective in ischemic stroke in mice (Kilic et al., 2008), and increased TLR4 expression is
131 associated with more severe stroke in patients (Yang et al., 2008).

132

133 Collectively, these studies suggest that naloxone can modulate immune and glial responses and
134 has therapeutic potential in stroke. However, its effects on post-stroke microglial activation and
135 recovery have not been studied. Since (+) and (-) forms have similar efficacy in reducing
136 microglial activation, the advantage of the (+)-form is that side effects from antagonizing opioid
137 receptors can be avoided. Thus, we aimed to study whether prolonged post-stroke administration
138 of (+)-naloxone in rats would promote recovery and whether this recovery is associated with

139 altered levels of activated microglia/macrophages. Furthermore, we took an approach of
140 intranasal administration since recent advances with intranasal naloxone formulations have
141 provided excellent bioavailability and enabled easy administration in patients. We first
142 characterized the neuroinflammatory response following focal cortical ischemia-reperfusion
143 injury since it is not well studied. As microglia/macrophages showed activation already on day 2
144 post-stroke in the ischemic cortex and maximum activation was observed at day 7, we
145 administered (+)-naloxone during this accumulation period. Here we show how post-stroke
146 intranasal (+)-naloxone promoted behavioral recovery during the short 14-day testing period, and
147 decreased microglia/macrophage activation and neuronal loss.

148

149 **Materials and Methods**

150 *Animals.* Adult male Sprague-Dawley rats (200-250 g, Charles River) were maintained under a
151 12h light-dark cycle. Food and water were freely available in the home cage. Experimental
152 procedures were approved by the NIDA Animal Care and Use Committee or by the National
153 Animal Experiment Board of Finland (protocol approval number ESAVI/5459/04.10.03/2011),
154 and followed the guidelines of the “Guide for the Care and Use of Laboratory Animals”
155 (National Institutes of Health publication, 1996), local laws and regulations.

156 *Cortical stroke model in rats with distal middle cerebral artery occlusion (dMCAo).* To
157 model focal cortical ischemic stroke in rats, the three-vessel occlusion method was used. In this
158 model, the stroke damage is restricted to the cortex, and the relative size of the stroke is close to
159 an average human stroke (Delavaran et al., 2013). Ligation of the right middle cerebral artery
160 (MCA) and common carotid arteries (CCAs) bilaterally was performed as described previously
161 (Airavaara et al., 2010; Airavaara et al., 2009; Chen et al., 1986; Harvey et al., 2011). Briefly,

162 rats were anesthetized with chloral hydrate 0.4 g/kg intraperitoneally (i.p.). The bilateral CCAs
163 were identified and isolated through a ventral midline cervical incision. The rats were placed in a
164 stereotaxic apparatus, and a craniotomy was performed to expose the right MCA. The MCA was
165 ligated with a 10-0 suture, and bilateral CCAs were ligated with non-traumatic arterial clamps.
166 After 60 or 90 minutes of ischemia, the suture around the MCA and arterial clips on CCAs were
167 removed to begin reperfusion. After recovery from anesthesia, the rats were returned to their
168 home cage. Body temperature during and after surgery was maintained at 37°C.

169 *Intranasal administration of (-)-naloxone and (+)-naloxone.* (-)-Naloxone and (+)-
170 naloxone were synthesized in the laboratory of Dr. Kenner Rice (NIDA IRP, NIH). Dosing was
171 estimated from a previously published study (Hutchinson et al., 2008). Drugs were administered
172 intranasally under isoflurane anesthesia (Anesthesia auto flow system, E-Z Anesthesia) starting
173 from post-stroke day 1, and were continued at 12-hour intervals for 7 days, a total of 14 times.
174 Briefly, animals were placed in the induction chamber for 1-1.5 minutes, and 5% isoflurane was
175 delivered at 1000cc/min. Animals were transferred to the nose cone where they received 1.5%
176 isoflurane delivered at 500cc/min for 30 seconds prior to intranasal naloxone delivery. To ensure
177 maximal delivery, animals remained in supine position during naloxone administration. When
178 the animals regained consciousness, they were returned to the home cage. Naloxone solution
179 was prepared fresh daily in sterile ultrapure water and stored at room temperature between
180 administrations. Using a Rainin LTS L-20 pipette and sterile pipette tips, 10 μ l of drug or vehicle
181 was administered into each nostril as described (Luo et al., 2013).

182 *Implantation of mini-osmotic pumps for continuous (+)-naloxone delivery.* Two days
183 following the dMCAo surgery the rats were anaesthetized with chloral hydrate (0.4 mg/kg i.p.)
184 for mini-osmotic pump implantation (Alzet, Palo Alto, CA, USA; model 2002). The pump was

185 implanted under the skin and the catheter was inserted into the right ventricle. The pumps were
186 filled with vehicle (sterile, ultrapure water) or (+)-naloxone 96 mg/ml. The pumping rate was 0.5
187 $\mu\text{l/h}$ and the pumps were left in place for 12 days.

188 *Behavioral analysis.* The elevated body swing test for body asymmetry (Borlongan et al.,
189 1998), modified Bederson's score (Bederson et al., 1986) and the measurement of locomotor
190 activity were performed as previously described (Airavaara et al., 2010; Airavaara et al., 2009).
191 Briefly, body asymmetry was analyzed from 20 consecutive trials by suspending the rats 20 cm
192 above the testing table by lifting their tails and counting the frequency of initial turnings of the
193 head or upper body contralateral to the ischemic side (the maximum impairment in stroke
194 animals is 20 contralateral turns whereas naïve animals turn in each direction with equal
195 frequency). For Bederson's score, neurological deficits were scored using the following criteria:
196 0 = rats extend both forelimbs straight when lifted by the tail, no observable deficit; 1 point =
197 rats keep the one forelimb to the breast and extend the other forelimb straight when lifted by the
198 tail; 2 points = rats show decreased resistance to lateral push in addition to behavior in score 1; 3
199 points = rats twist the upper half of their body when lifted by the tail in addition to behavior in
200 other scores. Locomotor activity was measured for 24h by placing the rat in a 42x42x31 cm
201 plexiglass box with an infrared activity monitor (Accuscan, Columbus, OH). All the behavioral
202 assessments were performed in a blinded manner and the experimenter did not know group
203 allocation. Body asymmetry and Bederson's score were assessed at the middle of the day, so that
204 the animals had fully recovered from isoflurane anesthesia needed for the period of intranasal
205 administration in the morning and in the evening.

206 *Histology.* The rats were deeply anaesthetized with pentobarbital (90 mg/kg i.p.) and
207 transcardially perfused with 200 ml saline followed by 500 ml of 4% paraformaldehyde. Brains

208 were processed for either paraffin or free-floating sections and stained with anti-Iba1, anti-CD68,
209 anti-NeuN, anti-GFAP, or anti-MBP antibodies.

210 *Immunostaining of paraffin sections.* Brains were post-fixed in 4% paraformaldehyde for
211 2 days, dehydrated in a series of ethanol and xylene, and embedded in paraffin. Brains were cut
212 into 5 μ m thick sagittal sections using a Leica HM355S microtome and mounted on Superfrost
213 Plus slides (Thermo Scientific, Waltham, MA). Sections were deparaffinized and antigen
214 retrieval was performed by heating in 0.05% citraconic anhydride (Sigma Aldrich, St. Louis,
215 MO), pH 7.4. Endogenous peroxidase activity was blocked with 0.6% hydrogen peroxide (Sigma
216 Aldrich), non-specific antibody binding was blocked with 1.5% normal goat or horse serum
217 (Vector Laboratories, Burlingame, CA), followed by incubation with primary antibody (rabbit
218 anti-Iba1 1:1000, cat#019-19741, RRID:AB_839504, Wako, Richmond, VA; mouse anti-CD68
219 1:500, cat#MCA341R, RRID:AB_2291300, AbD Serotec, Kidlington, UK; mouse anti-GFAP
220 1:1000, cat#MAB360, RRID:AB_2109815, Millipore, Billerica, MA; mouse anti-NeuN 1:200,
221 cat#MAB377, RRID:AB_2298772, Millipore; rabbit anti-MBP 1:500, cat#ab40390,
222 RRID:AB_1141521, Abcam, Cambridge, UK) at 4°C overnight. The next day, sections were
223 incubated with secondary antibody (goat anti-rabbit, RRID:AB_2336820, or horse anti-mouse,
224 RRID:AB_2336811, biotinylated secondary antibody 1:200, Vector Laboratories) followed by
225 incubation with avidin-biotin complex (ABC kit, Vector Laboratories). Color was developed
226 using peroxidase reaction with 3',3'-diaminobenzidine (DAB; RRID:AB_2336382, Vector
227 Laboratories). Cresyl violet staining was used as background staining with anti-CD68. For
228 immunofluorescence staining, goat anti-rabbit Alexa488 (1:500, cat#A11034,
229 RRID:AB_2576217, Life Technologies, Paisley, UK) and goat anti-mouse Alexa568 (1:500,
230 cat#A11004, RRID:AB_2534072, Life Technologies) were used as secondary antibodies.

231 *Immunostaining of free-floating sections.* Brains were dehydrated in 30% sucrose at 4°C
232 and sectioned coronally into 40 µm thick slices using a Leica CM3050 Cryostat. Sections were
233 taken from 2.1 to -1.0 mm (striatum) and -2.4 to -4.0 mm (thalamus) relative to bregma, then
234 stored in 1x PBS for short-term storage, or cryopreservant for long-term storage (20% glycerol,
235 2% DMSO in 1x PBS). Sections were blocked with 0.3% hydrogen peroxidase and 4% bovine
236 serum albumin (Sigma Aldrich) + 0.3% Triton-x-100 (Sigma Aldrich), then incubated with
237 primary antibody (rabbit anti-Iba1 1:2000, RRID:AB_839504; mouse anti-NeuN 1:1000,
238 RRID:AB_2298772) overnight at 4°C. The following day, sections were incubated with
239 secondary antibody, followed by incubation with avidin-biotin complex and DAB as above.

240 *Unbiased stereological counting of Iba1+ cells in the striatum.* Iba1-positive (Iba1+)
241 cells in the striatum were counted from 40 µm thick free-floating sections using unbiased
242 stereology with a stereomicroscope (Olympus BX51) and StereoInvestigator 6 program (MBF
243 Bioscience) as previously described (Mijatovic et al., 2007). The optical fractionator method,
244 which involves a three-dimensional probe for counting the cell of interest by randomly and
245 systematically sampling each section, was used. It is unbiased since it does not involve cell size
246 and shape, and is unaffected by tissue processing. Cell population is computed from the volume
247 fraction. The volume fraction consists of information on the thickness of tissue sampled, the
248 number of sections sampled, and the area in each section sampled. Three 40 µm thick coronal
249 slices were selected based on their relative location to bregma (+0.2, -0.26, and -0.4/-0.5 mm) to
250 obtain results relatively free of bias in the distribution of the cells. Only Iba1+ cells with clear
251 microglia morphology were counted. The contralateral and ipsilateral striata were first traced,
252 and then the area was analyzed for each slice. Approximately 60 to 80 randomly selected sites
253 per area/slice were analyzed to ensure accuracy and minimize error.

254 *Analysis of CD68+, Iba1+, and NeuN+ cells in the thalamus.* The number of CD68+,
255 Iba1+ and NeuN+ cells in the thalamus was analyzed using Image-Pro Analyzer 7.0 program.
256 Slides were scanned with a 3DHISTECH Panoramic 250 FLASH II digital slide scanner
257 (Budapest, Hungary; scanning service provided by the Institute of Biotechnology, University of
258 Helsinki; <http://www.biocenter.helsinki.fi/bi/histoscanner/index.html>) and 10x magnification
259 images of the thalamus were taken with Panoramic Viewer version 1.15.3. To estimate the
260 number of immunopositive cells in the ipsilateral thalamus, the thalamus was traced and the Iba1
261 immunoreactive area was counted from 3-6 coronal sections (in 3 rats there were only 2 sections
262 counted). The object count of NeuN+ cells in the thalamus was counted from 4-6 coronal
263 sections per brain. Sections were taken every 300-400 μm between -2.4 and -4.0 mm relative to
264 bregma, and an average for each brain was used for further analysis. The average number of
265 NeuN+ cells and the Iba1 immunoreactive area are expressed as a percentage compared to the
266 contralateral side. To estimate the number of CD68+ cells in the thalamus, the object count of
267 CD68+ cells was analyzed from 3-4 sagittal sections per hemisphere, taken every 500 μm
268 between 1.9 and 3.4 mm or -1.9 and -3.4 mm relative to bregma, and the average cell count per
269 hemisphere was used for further analysis.

270 *Quantitation of infarction size.* At day 14 post-stroke, the average infarction size was
271 quantified from 6 anti-NeuN stained coronal brain sections, taken every 800 μm between 1.80
272 and -3.00 mm relative to bregma. The area devoid of NeuN+ cells and the total area of the brain
273 section were defined in Panoramic Viewer version 1.15.3. Infarction size is expressed as a
274 percentage of the total area of the section. At day 2 post-stroke, the infarction volume was
275 quantified with 2,3,5-triphenyltetrazolium chloride (TTC) staining from 2 mm brain slices as
276 described previously (Airavaara et al., 2009).

277 *Measurement of TNF- α secretion from microglia/macrophages isolated from the stroke*
278 *cortex.* The CD11b immunopositive cortical microglia/macrophages were isolated by magnetic
279 activated cell sorting (MACS). The rats were anesthetized with pentobarbital (90 mg/kg i.p.) at 7
280 days post-stroke after 90 min dMCAo, and perfused with 200 ml of saline. The ischemic cortex
281 and the corresponding contralateral cortex were dissected on ice in HBSS without Ca²⁺ and
282 Mg²⁺. The tissue was dissociated using Neural tissue dissociation kit (T) (Miltenyi Biotec, San
283 Diego, CA, USA) and the gentleMACS Dissociator (Miltenyi Biotec). After dissociation, the
284 cells were suspended in 0.5% BSA in PBS and incubated with Myelin Removal Beads II (1:10,
285 Miltenyi Biotec) for 15 minutes at 4°C. The cells were washed and resuspended in 0.5% BSA in
286 PBS and filtered through an LS column (Miltenyi Biotec) using a QuadroMACS Separator
287 (Miltenyi Biotec). The total effluent was collected and resuspended in 0.5% BSA with 2 mM
288 EDTA in PBS. The cells were incubated at 4°C for 10 minutes with mouse anti-CD11b:FITC
289 antibody (1:10, cat# MCA275FA, RRID:AB_2129486, AbD Serotec). The cells were washed,
290 resuspended in 0.5% BSA with 2 mM EDTA in PBS and incubated with anti-FITC MicroBeads
291 (1:10, RRID:AB_244371, Miltenyi Biotec) for 15 minutes at 4°C. The cells were washed and
292 resuspended in 0.5% BSA with 2 mM EDTA in PBS. The cell suspension was applied to an LS
293 column placed on a QuadroMACS Separator, and the magnetically labeled cells were used for
294 further experiments. The cells were plated on poly-ornithin-coated glass coverslips on a 48-well
295 plate in the density of 30 000 cells/well in DMEM:F12 medium (Life Technologies) containing
296 10% FBS and 0.2% primocin (Invivogen, San Diego, CA). LPS or naloxone were added
297 immediately after the plating. The culture medium was collected 20h later and analyzed using
298 the Rat TNF alpha ELISA Ready-SET-Go!® kit (cat#88-7340-22, RRID:AB_2575088,
299 eBioscience, San Diego, CA). The results are presented from three independent experiments. The

300 CD11b+ cells were isolated from 2-3 rats in each experiment. The values for each well within an
301 experiment were normalized to the mean value of the control wells within the corresponding
302 experiment.

303 *Experimental Design and Statistical Analysis.* All the experiments and analyses were
304 performed in a blinded manner. First, the time course of glial activation in the dMCAo model
305 was characterized. To minimize the number of animals needed (n=24 in total; n=4 per group), 90
306 min occlusion time was used to create a robust lesion. Immunostaining of sagittal sections with
307 anti-Iba1, anti-CD68 and anti-GFAP antibodies was used to visualize the temporal and spatial
308 distribution of glial cells post-stroke. As the dMCAo model is unilateral, the contralateral
309 hemisphere was used as a control after we confirmed that the expression of glial cells in naïve
310 brain is similar to the contralateral hemisphere of ischemic brain. For quantitation of CD68+
311 cells, 3-4 sections per animal per hemisphere were used to result in an average.

312 Second, to test the efficacy of post-stroke (+)-naloxone (0.32 mg/kg; n=27), repeated
313 dosing (twice a day for 7 days) was used due to the short half-life of naloxone. To make the
314 setting clinically relevant, the treatment was started one day after stroke and was given
315 intranasally, and a smaller infarct using 60 min dMCAo was induced. Behavioral recovery was
316 monitored for 14 days with body asymmetry test, Bederson's score and measurement of
317 spontaneous locomotor activity. Vehicle (n=25) and no treatment groups (n=13) were used as a
318 control in the behavioral assays. As both naloxone enantiomers have anti-inflammatory effects
319 on microglia, only the (-) form antagonizes opioid receptors. Thus, we included also (-)-naloxone
320 (n=7) group in the behavioral assays to provide information whether (+)- and (-)-naloxone have a
321 similar effect on recovery. Dose-response of (+)-naloxone was tested in a separate experiment
322 (0.0008 mg/kg: n=8; 0.008 mg/kg: n=8; 0.08 mg/kg: n=7; 0.8 mg/kg: n=8; vehicle: n=11). The

323 amount of microglial activation in the striatum and thalamus, and neuronal loss in the cortex and
 324 thalamus were analyzed with immunohistochemistry. For quantitation of Iba1+ and NeuN+ cells,
 325 3-6 sections from corresponding coronal planes from each animal were used.

326 Statistical analyses were performed with IBM SPSS Statistics software version 24.0.
 327 Normal distribution of each dataset was analyzed by Levene's test for equality of variances and
 328 analyzed with either one-way ANOVA or Kruskal-Wallis nonparametric ANOVA, or with
 329 Student's t-test or nonparametric Mann-Whitney U test in the case of only two groups. One-way
 330 ANOVA was followed by Bonferroni's or Dunnett's post hoc test and Kruskal-Wallis test was
 331 followed by pairwise comparison with Mann-Whitney U test. Since the immunohistochemical
 332 data did not differ between the vehicle and no treatment groups or between (+)-naloxone doses
 333 0.32 mg/kg and 0.8 mg/kg, the two groups were combined as one control group and one (+)-
 334 naloxone group. Statistical significance was considered at $p < 0.05$. The results are presented as
 335 mean \pm standard error of the mean.

336

337 **Table 1: Statistical table**

	Dataset	Data structure	Type of test	Power
a	Fig. 2P	Non-normal distribution (unequal variances)	Kruskal-Wallis test, Mann-Whitney U	H(11)=41.5, $p=0.000$ Ipsilateral hemisphere: d2 vs. d7: $p=0.021$ d2 vs. d14: $p=0.021$ d2 vs. d28: $p=0.021$ d2 vs. d56: $p=0.021$ d2 vs. d112: $p=0.021$ d7 vs. d14: $p=0.021$ d7 vs. d28: $p=0.021$ d7 vs. d56: $p=0.083$ d7 vs. 112: $p=0.083$ d14 vs. d28: $p=1.00$ d14 vs. d56: $p=0.043$ d14 vs. d112: $p=0.021$

			d28 vs. d56: p=0.083 d28 vs. d112: p=0.043 d56 s. d112: p=0.773 Ipsilateral vs. contralateral: d2: p=0.773 d7: p=0.021 d14: p=0.021 d28: p=0.021 d56: p=0.021 d112: p=0.021	
b	Fig. 5B	Non-normal distribution	Kruskal-Wallis test, Mann-Whitney U	d1: H(2)= 2.26, p=0.323 d3: H(2)=4.93, p=0.085 d7: H(2)=1.29, p=0.524 d10: H(2)=15.5, p=0.000 NT vs. (+)-Nal: p=0.006 Veh vs. (+)-Nal: p=0.000 NT vs. Veh: p=0.651 d14: H(2)=12.3, p=0.002 NT vs. (+)-Nal: p=0.012 Veh vs. (+)-Nal: p=0.001 NT vs. Veh: p=0.485
c	Fig. 5C	Non-normal distribution	Kruskal-Wallis test, Mann-Whitney U	d1: H(2)= 3.25, p=0.197 d3: H(2)=6.92, p=0.032 NT vs. (+)-Nal: p=0.017 Veh vs. (+)-Nal: p=0.059 NT vs. Veh: p=0.393 d7: H(2)=3.26, p=0.196 d10: H(2)=15.4, p=0.000 NT vs. (+)-Nal: p=0.002 Veh vs. (+)-Nal: p=0.002 NT vs. Veh: p=0.203 d14: H(2)=19.1, p=0.000 NT vs. (+)-Nal: p=0.000 Veh vs. (+)-Nal: p=0.000 NT vs. Veh: p=0.209
d	Fig. 5D	Non-normal distribution	Kruskal-Wallis test, Mann-Whitney U	H(4)=15.1, p=0.004 Veh vs. $8 \cdot 10^{-4}$: p=0.206 Veh vs. $8 \cdot 10^{-3}$: p=0.966 Veh vs. $8 \cdot 10^{-2}$: p=0.002 Veh vs. $8 \cdot 10^{-1}$: p=0.059 $8 \cdot 10^{-4}$ vs. $8 \cdot 10^{-3}$: p=0.552 $8 \cdot 10^{-4}$ vs. $8 \cdot 10^{-2}$: p=0.001 $8 \cdot 10^{-4}$ vs. $8 \cdot 10^{-1}$: p=0.019 $8 \cdot 10^{-3}$ vs. $8 \cdot 10^{-2}$: p=0.031 $8 \cdot 10^{-3}$ vs. $8 \cdot 10^{-1}$: p=0.142 $8 \cdot 10^{-2}$ vs. $8 \cdot 10^{-1}$: p=0.488

e	Fig. 5E	Non-normal distribution	Kruskal-Wallis test, Mann-Whitney U	H(4)=6.38, p=0.041 Veh vs. $8 \cdot 10^{-4}$: p=0.690 Veh vs. $8 \cdot 10^{-3}$: p=0.487 Veh vs. $8 \cdot 10^{-2}$: p=0.016 Veh vs. $8 \cdot 10^{-1}$: p=0.038 $8 \cdot 10^{-4}$ vs. $8 \cdot 10^{-3}$: p=0.314 $8 \cdot 10^{-4}$ vs. $8 \cdot 10^{-2}$: p=0.006 $8 \cdot 10^{-4}$ vs. $8 \cdot 10^{-1}$: p=0.025 $8 \cdot 10^{-3}$ vs. $8 \cdot 10^{-2}$: p=0.144 $8 \cdot 10^{-3}$ vs. $8 \cdot 10^{-1}$: p=0.208 $8 \cdot 10^{-2}$ vs. $8 \cdot 10^{-1}$: p=0.730
f	Fig. 5F	Normal distribution	One-way ANOVA, Bonferroni	F(2,42)=0.054 NT vs. (+)-Nal: p=0.064 Veh vs. (+)-Nal: p=0.242 NT vs. Veh: p=1.00
g	Fig. 5G	Non-normal distribution (unequal variances)	Kruskal-Wallis test, Mann-Whitney U	H(2)=6.82, p=0.033 NT vs. (+)-Nal: p=0.004 Veh vs. (+)-Nal: p=0.243 NT vs. Veh: p=0.313
h	Fig. 5H	Non-normal distribution	Mann-Whitney U	d1: p=0.663 d3: p=0.663 d7: p=0.963 d10: p=0.001 d14: p=0.000
i	Fig. 5I	Non-normal distribution	Mann-Whitney U	d1: p=0.159 d3: p=0.401 d7: p=0.565 d10: p=0.002 d14: p=0.005
j	Fig. 5J	Normal distribution	t-test	d7: t(16)=0.47, p=0.647 d14: t(16)=0.06, p=0.953
k	Fig. 5K	Normal distribution	One-way ANOVA, Bonferroni	d7: F(2,59)=5.27, p=0.008 NT vs. (+)-Nal: p=0.574 Veh vs. (+)-Nal: p=0.113 NT vs. Veh: p=0.009 d14: F(2,62)=1.79, p=0.175
l	Fig. 6A	Normal distribution	t-test	t(26)=2.51, p=0.019
m	Fig. 6B	Non-normal distribution (unequal variances)	Kruskal-Wallis test, Mann-Whitney U	H(2)=11.4, p=0.003 Naïve vs. Ctrl: p=0.002 Naïve vs. (+)-Nal: p=0.157 Ctrl vs. (+)-Nal: p=0.036
n	Fig. 7A	Normal distribution	One-way ANOVA, Bonferroni	F(2,31)=8.63, p=0.001 Naïve vs. Ctrl: p=0.003 Naïve vs. (+)-Nal: p=1.00

				Ctrl vs. (+)-Nal: p=0.013
o	Fig. 7B	Non-normal distribution (unequal variances)	Kruskal-Wallis test, Mann-Whitney U	H(2)=5.77, p=0.056
p	Fig. 7C	Non-normal distribution (unequal variances)	Kruskal-Wallis test, Mann-Whitney U	H(2)=17.6, p=0.000 Naïve vs. Ctrl: p=0.000 Naïve vs. (+)-Nal: p=0.001 Ctrl vs. (+)-Nal: p=0.027
q	Fig. 8B	Normal distribution	t-test	t(13)=0.89, p=0.389
r	Fig. 8D	Non-normal distribution	Mann-Whitney U	d2: p=0.861 d6: p=0.825 d10: p=0.279 d16: p=0.066
s	Fig. 8F	Non-normal distribution	Mann-Whitney U	d1: p=0.800 d3: p=0.861 d7: p=0.516 d10: p=0.391 d14: p=0.694
t	Fig. 8G	Normal distribution	Two-way RM ANOVA	F(4,52)=0.29, p=0.88
u	Fig. 9A	Non-normal distribution (unequal variances)	Mann-Whitney U	p=0.006
v	Fig. 9B	Normal distribution	One-way ANOVA, Dunnett	F(6,54)=2.74, p=0.022 20 μ M (-)-Nal: p=0.669 50 μ M (-)-Nal: p=0.020 100 μ M (-)-Nal: p=0.218 20 μ M (+)-Nal: p=0.492 50 μ M (+)-Nal: p=0.637 100 μ M (+)-Nal: p=0.006

338 d = post-stroke day; NT = no treatment; (+)-Nal = (+)-naloxone; Veh = vehicle; Ctrl = control; (-

339)-Nal = (-)-naloxone; RM = repeated measures

340

341 Results

342 Long-lasting microglial and astrocyte activation in the ipsilateral hemisphere after dMCAo

343 We first characterized the neuroinflammatory response in proximal (cortex) and distal (thalamus)

344 regions following transient 90 min dMCAo, and second, tested the efficacy of post-stroke

345 intranasal naloxone treatment in adult rats after 60 min dMCAo. At day 2 post-stroke,

346 microglia/macrophage activation was observed mainly in the peri-infarct region, and few

347 phagocytic CD68+ (a marker for activated, phagocytic microglia/macrophages) cells were
348 present (Fig. 2C-D). Microglia/macrophage activation peaked on day 7 post-stroke in the
349 ischemic cortex when the core area was filled with Iba1+ (a marker for all
350 microglia/macrophages) and CD68+ cells having a phagocytic/macrophage-type morphology
351 (Fig. 2Ea, Fa). Microglia/macrophage activation was seen in the ipsilateral striatum starting from
352 post-stroke day 7 (Fig. 2Ec). Interestingly, activated microglia/macrophages were aligned along
353 fiber bundles, with a “stream-like” formation along the myelin embedded axons (Fig. 3). Iba1+
354 cells with activated morphology were evident in the ipsilateral thalamus at day 7 post-stroke, but
355 only a few cells were CD68+ (Fig. 2Ed, Fd, P). CD68 immunoreactivity increased in the
356 ipsilateral thalamus after post-stroke day 7, peaked at days 14-28, and remained elevated until
357 day 112 ($H(11)=41.5$, $p<0.001$, Kruskal-Wallis, Table 1a; Fig. 2P). These results suggest that
358 inflammation in the thalamus is long lasting and phagocytic cells are present in far distal areas at
359 least 4 months after stroke (Fig. 2Nd, P). Neuronal loss was observed in the ipsilateral thalamus
360 at post-stroke day 14 (Fig. 6B). At 112 days post-stroke, atrophy of the thalamus due to
361 shrinkage of the ipsilateral thalamus was observed (Fig. 2Me, Ne, Fig. 4Ge). Analysis of
362 spatiotemporal activation of GFAP+ cells (a marker for astrocytes) revealed a similar pattern as
363 microglia/macrophage activation (Fig. 4). Similarly to microglia, astrocytes in the ischemic core
364 died during the first couple of days. Astrogliosis was found in the peri-infarct area starting from
365 day 2 post-stroke (Fig. 4Bb). There was clear astrocytic scar formation in the peri-infarct region
366 starting from post-stroke day 7 (Fig. 4Cb, Ce). From day 7 onwards, astrogliosis was evident in
367 the striatum and even in the thalamus (Fig. 4C-G). Astrogliosis in the ipsilateral thalamus
368 persisted for up to 112 days post-stroke (Fig. 4Gd, Ge), suggesting glial scar formation without
369 local ischemic damage.

370

371 **Post-stroke treatment with intranasal (+)-naloxone started on day 1 post-stroke promotes**
372 **short-term behavioral recovery, reduces neuronal loss and decreases microglial activation**

373 The efficacy of post-stroke (+)-naloxone treatment was tested in rats (n=65), and treatment was
374 initiated one day after 60 min dMCAo, before extensive activation of microglia/macrophages,
375 and it was continued for 7 days i.e. the period when microglia/macrophage activation progresses
376 in the ischemic region. One day post-stroke, the rats were balanced into groups based on their
377 neurological deficits as measured by body asymmetry and Bederson's score, and (+)-naloxone
378 (0.32 mg/kg) or vehicle were administered intranasally every 12h for 7 days (i.e. 14 doses per
379 animal, Fig. 5A). To identify the confounding effect of isoflurane, two control groups were
380 included: (i) stroke rats receiving intranasal vehicle (including repeated isoflurane) and (ii) stroke
381 rats with no intranasal treatment and no isoflurane. There were no significant differences in body
382 asymmetry amongst the groups on days 1, 3, or 7 after dMCAo (Fig. 5B, Table 1b). However, on
383 days 10 and 14 post-stroke, body asymmetry ($H(2)=15.5$, $p<0.001$ and $H(2)=12.3$, $p=0.002$,
384 respectively, Kruskal-Wallis, Table 1b) and neurological deficits ($H(2)=15.4$, $p<0.001$ and
385 $H(2)=19.1$, $p<0.001$, respectively, Table 1c) were significantly reduced in the (+)-naloxone
386 treated rats (Fig. 5B-C). The reduction in body asymmetry ($H(4)=15.1$, $p=0.004$, Kruskal-Wallis,
387 Table 1d) and neurological deficits ($H(4)=6.38$, $p=0.041$, Table 1e) was dose-dependent (Fig.
388 5D-E). As another indicator of hastened recovery, (+)-naloxone improved locomotor activity at
389 day 14 post-stroke ($H(2)=6.82$, $p=0.033$, Kruskal-Wallis, Table 1g; Fig. 5G). Similarly, (-)-
390 naloxone (0.32 mg/kg, intranasally) induced behavioral recovery on days 10 and 14 post-stroke
391 (n=18) ($p=0.001$ and $p<0.001$, respectively, for body asymmetry test, Table 1h; and $p=0.002$ and
392 $p=0.005$, respectively, for Bederson's score, Mann-Whitney U-test, Table 1i; Fig. 5H-I). It has

393 been reported that continuous administration of the opioid receptor antagonist (-)-naltrexone
394 decreases body weight and appetite (Atkinson, 1984). We found no effect on the body weight
395 with naloxone treatment (Table 1j-k, Fig. 5J-K).

396

397 Post-stroke (+)-naloxone (0.32-0.8 mg/kg) reduced infarction size on day 14 after dMCAo
398 ($t(26)=2.51$, $p=0.019$, unpaired t-test, Table 1i; Fig. 6A) and prevented delayed neuronal death in
399 the ipsilateral thalamus ($H(2)=11.4$, $p=0.003$, Kruskal-Wallis, Table 1m; Fig. 6B). We observed
400 a negative correlation between the number of neurons (NeuN+ cells) in the ipsilateral thalamus
401 and infarction size (Pearson correlation $R = -0.691$, $p < 0.0001$), showing that the larger the
402 lesion in the cortex, the more extensive neuronal loss in the thalamus. (+)-Naloxone significantly
403 decreased the Iba1+ cell number in the ipsilateral striatum at post-stroke day 14 ($F(2,31)=8.63$,
404 $p=0.001$, one-way ANOVA, Table 1n; Fig. 7A). There was no statistical difference in the
405 contralateral striatum (Table 1o, Fig. 7B). Similarly, a significant reduction of Iba1
406 immunoreactivity by (+)-naloxone was found in the ipsilateral thalamus ($H(2)=17.6$, $p<0.001$,
407 Kruskal-Wallis, Table 1p; Fig. 7C).

408

409 **Pre-treatment or delayed post-stroke treatment with (+)-naloxone is not beneficial in** 410 **dMCAo model**

411 We tested the neuroprotective effect of (+)-naloxone ($n=15$) by giving (+)-naloxone (0.32
412 mg/kg) or vehicle intranasally three times: 12h and 1h before 60 min dMCAo and immediately
413 after reperfusion (Fig. 8A). The infarction volume was determined by TTC staining 2 days after
414 stroke. We found no significant differences in the infarction volume between the groups
415 ($p=0.389$, unpaired t-test, Table 1q; Fig. 8B). To answer the question whether more delayed (+)-

416 naloxone treatment would give similar effect on recovery as the treatment started on post-stroke
417 day 1, we administered (+)-naloxone (0.8 mg/kg) or vehicle intranasally twice daily starting from
418 day 3 after 60 min dMCAo and continuing for 7 days (n=13; Fig. 8C). There was an evident
419 recovery effect over time in the body asymmetry test, but there were no statistically significant
420 differences between the vehicle and (+)-naloxone groups (Table 1r; Fig. 8D). On post-stroke day
421 16, there was a tendency ($p=0.066$, Mann-Whitney U test, Table 1r) in the (+)-naloxone group
422 for milder neurological deficits in the body asymmetry test, but it did not reach statistical
423 significance. To study whether longer, continuous administration of (+)-naloxone would further
424 enhance recovery after 60 min dMCAo, we delivered (+)-naloxone (1.15 mg/24 h) or vehicle
425 into the ventricle using mini-osmotic pumps from post-stroke day 2 until post-stroke day 14
426 (n=15; Fig. 8E). There was again evident recovery effect in the body asymmetry test, but there
427 were no differences between the vehicle and (+)-naloxone groups (Table 1s; Fig. 8F). Nor were
428 there any differences in the body weight between the groups (Table 1t; Fig. 8G).

429

430 **Naloxone decreases TNF- α secretion from microglia/macrophages**

431 To test whether naloxone enantiomers affect cytokine secretion, we isolated CD11b+
432 microglia/macrophages from the infarct area at day 7 post-stroke and measured the secretion of
433 TNF- α , a cytokine with well-characterized pro-inflammatory effect downstream of TLR4
434 signaling. First, we tested whether the isolated cells respond to treatment with LPS by increasing
435 the secretion of TNF- α . Overnight treatment with LPS increased the amount of secreted TNF- α
436 approximately 3.5-fold ($p=0.006$, Mann-Whitney U, Table 1u; Fig. 9A), confirming that the
437 isolated cell population had properties characteristic of microglia and macrophages. Overnight
438 treatment with both naloxone enantiomers decreased the amount of TNF- α in the culture medium

439 statistically significantly ($F(6,54)=2.74$, $p=0.022$, one-way ANOVA, Table 1v; Fig. 9B). (-)-
440 Naloxone 50 μM and (+)-naloxone 100 μM decreased the unstimulated secretion of TNF- α by
441 approximately 15% compared to the control.

442

443 **Discussion**

444 We show for the first time that intranasal post-stroke administration of naloxone enantiomers
445 reduces inflammation and hastens recovery during short-term behavioral monitoring. Our data
446 support a therapeutic window for initiation of twice daily (+)-naloxone treatment between 16-
447 36h post-stroke and continuing the treatment for 7 days. Our study also indicates that modulation
448 of microglia/macrophage activation in the ischemic cerebral cortex and remote regions in the
449 striatum and thalamus is a potential therapeutic drug strategy. Since microglia/macrophages can
450 phagocytose viable neurons after ischemia (Neher et al., 2013), neuroinflammation may lead to
451 secondary neuronal loss. An ischemic brain injury leads to activation of microglia, the release of
452 pro-inflammatory factors, and further potentiates neuronal damage days to weeks after dMCAo
453 (Dirnagl et al., 1999). It has been suggested, that during an ischemic event the brain remains in a
454 continual state of neurotoxicity and microglia become over-activated, releasing pro-
455 inflammatory factors that can contribute to further damage (Glass et al., 2010). It is known that
456 over-reactive microglia can cause increased levels of cytokines, specifically TNF- α and
457 interleukin-1 β and -6 (Block et al., 2007; Lee et al., 1993). Therefore anti-inflammatory drugs,
458 such as minocycline, have been used to alleviate this neuroinflammation and improve stroke
459 outcome (Yrjanheikki et al., 1999). Liebigt *et al.* have shown that post-stroke application of
460 minocycline and indomethacin in rats, combined with rehabilitative training, produces improved
461 functional recovery compared to training alone (Liebigt et al., 2012).

462

463 Our data indicate that twice a day post-stroke treatment with (+)-naloxone for a week improves
464 short-term behavioral recovery and reduces neuronal damage and infarction size. The behavioral
465 effect of (+)-naloxone correlated with suppression of activated microglia in the striatum and
466 thalamus and was not observed until day 10 post-stroke, which suggests that (+)-naloxone targets
467 delayed post-stroke pathophysiological mechanisms such as inflammation. The administration of
468 (+)-naloxone was targeted to the period when the number of activated microglia/macrophages is
469 peaking in the cerebral cortex and before microglial activation is evident in the striatum or
470 thalamus. We, therefore, propose that dampening microglia/macrophage activation with post-
471 stroke (+)-naloxone restricts inflammation to limit associated lesion-expansion that occurs up to
472 24-48h after transient MCAo (Li et al., 2000; Liu et al., 2009). This is further supported by the
473 fact that (+)-naloxone treatment starting on days 2-3 post-stroke did not have a significant effect
474 on recovery. Thus, the therapeutic window for (+)-naloxone seems to be between 16-36h post-
475 stroke when there is not yet substantial activation of microglia. However, when using mini-
476 osmotic pumps the drug kinetics and concentrations at the target tissues over the administration
477 period are only estimations until quantitative assessments of delivery are performed. When the
478 intranasal (+)-naloxone treatment was started at day 3 post-stroke and continued for 7 days, there
479 was a trend for milder neurological deficits on day 16 post-stroke ($p=0.066$). Due to the small
480 number of animals, the data is inconclusive and further studies are needed to fully optimize the
481 dosing and timing of administration. Yet, pre-stroke treatment with (+)-naloxone was not
482 neuroprotective as has been shown before by Liao *et al.* (Liao et al., 2003), and supports our
483 hypothesis that (+)-naloxone should be administered during the inflammation period.

484

485 We also show that naloxone enantiomers decrease unstimulated TNF- α secretion from
486 microglia/macrophages isolated from the stroke cortex at day 7 post-stroke. Although the
487 characteristics and phenotypes of microglia are altered in *in vitro* conditions (Gosselin et al.,
488 2017), this data strengthen the view that (+)-naloxone can regulate the pro-inflammatory
489 function of microglia/macrophages. Moreover, microglia phenotype is highly dependent on the
490 environment where it is and therefore the data should be interpreted carefully. It is noteworthy
491 though that this study is the first to show that (-)- or (+)-naloxone inhibits basal TNF- α secretion
492 from stroke-activated microglia/macrophages without extra stimulus.

493

494 The time course of microglial and astrocyte activation in the thalamus following cortical stroke is
495 less studied. We observed activated microglia/macrophages and increased GFAP
496 immunoreactivity in the thalamus still at 4 months post-stroke, and indeed, also in the
497 intraluminal MCAo model microglial activation in the thalamus has been reported to be long-
498 lasting, for up to 6 months post-stroke (Justicia et al., 2008). However, in the intraluminal MCAo
499 model the ischemic lesion is somewhat close to the thalamus and in some cases extends into it.
500 Microglia and astrocytes have been shown to be activated already after day 3 post-stroke in the
501 ipsilateral thalamus in the transient intraluminal MCAo model (Loos et al., 2003). In our model,
502 microglial and astrocyte activation was evident in the ipsilateral thalamus at 7 days post-stroke,
503 but interestingly, microglia were not phagocytic until at day 14. Previously, it has been reported
504 that neuronal degeneration in the ipsilateral thalamus is evident at 14 days post-stroke in the
505 transient intraluminal MCAo model (Loos et al 2003), similar to our findings. The ischemia-
506 induced neuronal loss and microglia/macrophage activation in the thalamus probably reflects
507 retrograde/anterograde degeneration caused by cortical damage. However, inflammation has

508 been implicated in secondary neurodegeneration (Block et al., 2005; Schroeter et al., 2006) and
509 (+)-naloxone reduces inflammation and neurodegeneration at both primary (cortex) and
510 secondary (thalamus) sites of injury. Although it remains unclear whether the beneficial effects
511 of (+)-naloxone occur directly in cells in the thalamus or indirectly by reducing inflammation in
512 the cortex, or both, intranasal (+)-naloxone is apparently beneficial to recovery from stroke. The
513 thalamus regulates multiple sensory and motor functions that are also controlled by other brain
514 regions. Furthermore, the thalamus is a relay-station connecting the right and left hemispheres,
515 and a unilateral lesion of the thalamus usually has little behavioral consequences (Carrera and
516 Bogousslavsky, 2006). Overall, the role of thalamic neurodegeneration and inflammation
517 following cortical infarction remains unclear, and it is not known whether the secondary
518 pathology affects the behavioral recovery. Our study supports the need for future research into
519 the role of thalamic injury in cortical stroke.

520

521 Single (+)-naloxone doses that had effect on recovery in our study were 0.08 mg/kg, 0.32 mg/kg
522 and 0.8 mg/kg. As a comparison, the FDA-approved Narcan[®] nasal spray to treat opioid
523 overdose contains 4 mg of (-)-naloxone hydrochloride being equivalent to 0.08 mg/kg dose for a
524 person weighing 50 kg. Based on pharmacokinetic data on naloxone (Dowling et al., 2008;
525 Krieter et al., 2016), we estimated that (+)-naloxone levels in rat brain reached nanomolar
526 concentrations. The pharmacokinetic profile of naloxone is favorable for stroke treatment since it
527 is efficiently transported to the brain. However, its short elimination half-life [1.57 ± 0.784 h
528 (Lewis et al., 2012)] requires repeated dosing. Short-term (up to 2 days post-stroke) intravenous
529 (-)-naloxone (dose from 0.4 mg to 4 mg) has been tested in patients having an acute ischemic
530 stroke, and it has rapidly, within minutes, improved neurological deficits (Baskin and Hosobuchi,

531 1981; Jabaily and Davis, 1984). However, later clinical studies on the efficacy of naloxone have
532 been inconclusive. A phase II open trial studying the safety of a high loading dose followed by
533 24h infusion of (-)-naloxone did not find benefit at 3 months post-stroke when the treatment was
534 started within 48h of stroke onset (Olinger et al., 1990). A subsequent double-blind, randomized
535 pilot trial using the 24h infusion found no significant differences between the naloxone and
536 placebo groups when the treatment was initiated within 12h of the onset of symptoms (Federico
537 et al., 1991). At the time when these studies were performed, the anti-inflammatory effects of
538 naloxone were not known. The lack of effect in these clinical studies may have resulted from the
539 short treatment regimen. Treatment for only 24h may not be enough to dampen the post-stroke
540 microglial response. Moreover, the clinical studies have been based on the assumption that
541 opioid antagonism is at least partly behind the beneficial effect of naloxone in acute stroke that
542 was reported in the early case studies in the 1980's. In our experiment, both (+)- and (-)-
543 naloxone had a similar effect on recovery starting from post-stroke day 10 onwards, implying
544 that opioid receptor antagonism is not necessary for the recovery promoting effect in the chronic
545 phase of stroke. Thus, we propose additional clinical studies that would employ different dosing
546 paradigms to optimize the post-stroke (+)-naloxone dosing regimen.

547

548 The Stroke Therapy Academic Industry Roundtable (STAIR) recommendations to improve the
549 quality of preclinical stroke studies emphasize the importance of dose-response and therapeutic
550 window studies together with histological and functional outcome monitoring. According to
551 STAIR recommendations, the therapies should be tested in several animal species using both
552 sexes as well as aged, and comorbid animals. Therefore, we warrant further studies using (+)-
553 naloxone for stroke treatment in female, aged and comorbid animals to better reflect the clinical

554 situation within the heterogeneous patient population. Also, behavioral testing should be carried
555 out for more than 14 days to confirm the beneficial effect of (+)-naloxone on long-term
556 behavioral recovery. Regarding the safety of naloxone therapy, naloxone has been already shown
557 to be safe and well tolerated in patients with the corresponding dose range we have been using in
558 rats.

559

560 In conclusion, characterization of the neuroinflammatory response in rat cortical stroke revealed
561 long-lasting microglia/macrophage and astrocyte activation as well as neuronal death in the
562 ipsilateral thalamus. Phagocytic cells were present in the thalamus for up to 4 months post-
563 stroke. This delayed neuronal loss and phagocytosis in the thalamus could serve as a new target
564 for drug treatment after stroke with a larger therapeutic window than exists for current post-
565 stroke treatment (i.e. tissue plasminogen activator). Most importantly, we found that intermittent
566 post-stroke intranasal (+)-naloxone treatment starting on day 1 post-stroke promoted short-term
567 behavioral recovery, reduced microglial activation in the striatum and thalamus, and decreased
568 neuronal loss in the cortex and thalamus. It is likely that (+)-naloxone mediates its positive
569 effects on stroke via mechanisms where TLR signaling and reduction of oxidative stress are
570 involved. (+)-Naloxone is thus a promising drug for the treatment of ischemic stroke.

571

572 **References**

573 Airavaara M, Chiocco MJ, Howard DB, Zuchowski KL, Peranen J, Liu C, Fang, S, Hoffer BJ,
574 Wang Y, Harvey BK (2010) Widespread cortical expression of MANF by AAV serotype 7:
575 localization and protection against ischemic brain injury. *Exp Neurol* 225: 104-113.

- 576 Airavaara M, Shen H, Kuo CC, Peranen J, Saarna M, Hoffer B, Wang Y (2009) Mesencephalic
577 astrocyte-derived neurotrophic factor reduces ischemic brain injury and promotes behavioral
578 recovery in rats. *J Comp Neurol* 515: 116-124.
- 579 Atkinson RL (1984) Endocrine and metabolic effects of opiate antagonists. *J Clin Psychiatry* 45:
580 20-24.
- 581 Baskin DS, Hosobuchi Y (1981) Naloxone reversal of ischaemic neurological deficits in man.
582 *Lancet* 2: 272-275.
- 583 Bederson JB, Pitts LH, Tsuji M, Nishimura MC, Davis RL, Bartkowski H (1986) Rat middle
584 cerebral artery occlusion: evaluation of the model and development of a neurologic examination.
585 *Stroke* 17: 472-476.
- 586 Block F, Dihne M, Loos M (2005) Inflammation in areas of remote changes following focal
587 brain lesion. *Prog Neurobiol* 75: 342-365.
- 588 Block ML, Zecca L, Hong JS (2007) Microglia-mediated neurotoxicity: uncovering the
589 molecular mechanisms. *Nat Rev Neurosci* 8: 57-69.
- 590 Borlongan CV, Tajima Y, Trojanowski JQ, Lee VM, Sanberg PR (1998) Cerebral ischemia and
591 CNS transplantation: differential effects of grafted fetal rat striatal cells and human neurons
592 derived from a clonal cell line. *Neuroreport* 9: 3703-3709.
- 593 Carrera E, Bogousslavsky J (2006) The thalamus and behavior: effects of anatomically distinct
594 strokes. *Neurology* 66: 1817-1823.
- 595 Chen CJ, Liao SL, Chen WY, Hong JS, Kuo JS (2001) Cerebral ischemia/reperfusion injury in
596 rat brain: effects of naloxone. *Neuroreport* 12: 1245-1249.
- 597 Chen ST, Hsu CY, Hogan EL, Maricq H, Balentine JD (1986) A model of focal ischemic stroke
598 in the rat: reproducible extensive cortical infarction. *Stroke* 17: 738-743.

599 Delavaran H, Sjunnesson H, Arvidsson A, Lindvall O, Norrving B, van Westen D, Kokaia Z,
600 Lindgren A (2013) Proximity of brain infarcts to regions of endogenous neurogenesis and
601 involvement of striatum in ischaemic stroke. *Eur J Neurol* 20: 473-479.

602 Dirnagl U (2012) Pathobiology of injury after stroke: the neurovascular unit and beyond. *Ann N*
603 *Y Acad Sci* 1268: 21-25.

604 Dirnagl U, Iadecola C, Moskowitz MA (1999) Pathobiology of ischaemic stroke: an integrated
605 view. *Trends Neurosci* 22: 391-397.

606 Dowling J, Isbister GK, Kirkpatrick CM, Naidoo D, Graudins A (2008) Population
607 pharmacokinetics of intravenous, intramuscular, and intranasal naloxone in human volunteers.
608 *Ther Drug Monit* 30: 490-496.

609 Endres M, Engelhardt B, Koistinaho J, Lindvall O, Meairs S, Mohr JP, Planas A, Rothwell N,
610 Schwaninger M, Schwab ME, Vivien D, Wieloch T, Dirnagl U (2008) Improving outcome after
611 stroke: overcoming the translational roadblock. *Cerebrovasc Dis* 25: 268-278.

612 Federico F, Lucivero V, Lamberti P, Fiore A, Conte C (1991) A double blind randomized pilot
613 trial of naloxone in the treatment of acute ischemic stroke. *Ital J Neurol Sci* 12: 557-563.

614 Glass CK, Saijo K, Winner B, Marchetto MC, Gage FH (2010) Mechanisms underlying
615 inflammation in neurodegeneration. *Cell* 140: 918-934.

616 Gosselin D, Skola D, Coufal NG, Holtman IR, Schlachetzki JCM, Sajti E, Jaeger BN, O'Connor
617 C, Fitzpatrick C, Pasillas MP, Pena M, Adair A, Gonda DD, Levy ML, Ransohoff RM, Gage
618 FH, Glass CK (2017) An environment-dependent transcriptional network specifies human
619 microglia identity. *Science* 356: eaal3222.

620 Harvey BK, Airavaara M, Hinzman J, Wires EM, Chiocco MJ, Howard DB, Shen H, Gerhardt
621 G, Hoffer BJ, Wang Y (2011) Targeted over-expression of glutamate transporter 1 (GLT-1)
622 reduces ischemic brain injury in a rat model of stroke. PloS one 6: e22135.

623 Hutchinson MR et al. (2012) Opioid activation of toll-like receptor 4 contributes to drug
624 reinforcement. J Neurosci 32: 11187-11200.

625 Hutchinson MR, Zhang Y, Brown K, Coats BD, Shridhar M, Sholar PW, Patel SJ, Crysdale NY,
626 Harrison JA, Maier SF, Rice KC, Watkins LR (2008) Non-stereoselective reversal of
627 neuropathic pain by naloxone and naltrexone: involvement of toll-like receptor 4 (TLR4). Eur J
628 Neurosci 28 20-29.

629 Iijima I, Minamikawa J, Jacobson AE, Brossi A, Rice KC (1978) Studies in the (+)-morphinan
630 series. 5. Synthesis and biological properties of (+)-naloxone. J Med Chem 21: 398-400.

631 Jabaily J, Davis JN (1984) Naloxone administration to patients with acute stroke. Stroke 15: 36-
632 39.

633 Justicia C, Ramos-Cabrer P, Hoehn M (2008) MRI detection of secondary damage after stroke:
634 chronic iron accumulation in the thalamus of the rat brain. Stroke 39: 1541-1547.

635 Kilic U, Kilic E, Matter CM, Bassetti CL, Hermann DM (2008) TLR-4 deficiency protects
636 against focal cerebral ischemia and axotomy-induced neurodegeneration. Neurobiol Dis 31: 33-
637 40.

638 Krieter P, Chiang N, Gyaw S, Skolnick P, Crystal R, Keegan F, Aker J, Beck M, Harris J (2016)
639 Pharmacokinetic Properties and Human Use Characteristics of an FDA-Approved Intranasal
640 Naloxone Product for the Treatment of Opioid Overdose. J Clin Pharmacol 56: 1243-1253.

- 641 Lee SC, Liu W, Dickson DW, Brosnan CF, Berman JW (1993) Cytokine production by human
642 fetal microglia and astrocytes. Differential induction by lipopolysaccharide and IL-1 beta. *J*
643 *Immunol* 150: 2659-2667.
- 644 Lehnardt S, Massillon L, Follett P, Jensen FE, Ratan R, Rosenberg PA, Volpe JJ, Vartanian T
645 (2003) Activation of innate immunity in the CNS triggers neurodegeneration through a Toll-like
646 receptor 4-dependent pathway. *PNAS* 100: 8514-8519.
- 647 Lewis SS, Loram LC, Hutchinson MR, Li CM, Zhang Y, Maier SF, Huang Y, Rice KC, Watkins
648 LR (2012) (+)-naloxone, an opioid-inactive toll-like receptor 4 signaling inhibitor, reverses
649 multiple models of chronic neuropathic pain in rats. *J Pain* 13: 498-506.
- 650 Li F, Silva MD, Sotak CH, Fisher M (2000) Temporal evolution of ischemic injury evaluated
651 with diffusion-, perfusion-, and T2-weighted MRI. *Neurology* 54: 689-696.
- 652 Liao SL, Chen WY, Raung SL, Chen CJ (2003) Neuroprotection of naloxone against ischemic
653 injury in rats: role of mu receptor antagonism. *Neurosci Lett* 345: 169-172.
- 654 Liebigt S, Schlegel N, Oberland J, Witte OW, Redecker C, Keiner S (2012) Effects of
655 rehabilitative training and anti-inflammatory treatment on functional recovery and cellular
656 reorganization following stroke. *Exp Neurol* 233: 776-782.
- 657 Liu B, Du L, Hong JS (2000a) Naloxone protects rat dopaminergic neurons against inflammatory
658 damage through inhibition of microglia activation and superoxide generation. *J Pharmacol Exp*
659 *Ther* 293: 607-617.
- 660 Liu B, Du L, Kong LY, Hudson PM, Wilson BC, Chang RC, Abel HH, Hong JS (2000b)
661 Reduction by naloxone of lipopolysaccharide-induced neurotoxicity in mouse cortical neuron-
662 glia co-cultures. *Neuroscience* 97: 749-756.

- 663 Liu B, Jiang JW, Wilson BC, Du L, Yang SN, Wang JY, Wu GC, Cao XD, Hong JS (2000c)
664 Systemic infusion of naloxone reduces degeneration of rat substantia nigral dopaminergic
665 neurons induced by intranigral injection of lipopolysaccharide. *J Pharmacol Exp Ther* 295: 125-
666 132.
- 667 Liu F, Schafer DP, McCullough LD (2009) TTC, fluoro-Jade B and NeuN staining confirm
668 evolving phases of infarction induced by middle cerebral artery occlusion. *J Neurosci Methods*
669 179: 1-8.
- 670 Liu Y, Qin L, Wilson BC, An L, Hong JS, Liu B (2002) Inhibition by naloxone stereoisomers of
671 beta-amyloid peptide (1-42)-induced superoxide production in microglia and degeneration of
672 cortical and mesencephalic neurons. *J Pharmacol Exp Ther* 302: 1212-1219.
- 673 Loos M, Dihne M, Block F (2003) Tumor necrosis factor-alpha expression in areas of remote
674 degeneration following middle cerebral artery occlusion of the rat. *Neuroscience* 122: 373-380.
- 675 Luo Y, Shen H, Liu HS, Yu SJ, Reiner DJ, Harvey BK, Hoffer BJ, Yang Y, Wang Y (2013)
676 CART peptide induces neuroregeneration in stroke rats. *J Cereb Blood Flow Metab* 33: 300-310.
- 677 Mijatovic J, Airavaara M, Planken A, Auvinen P, Raasmaja A, Piepponen TP, Costantini F,
678 Ahtee L, Saarna M (2007) Constitutive Ret activity in knock-in multiple endocrine neoplasia
679 type B mice induces profound elevation of brain dopamine concentration via enhanced synthesis
680 and increases the number of TH-positive cells in the substantia nigra. *J Neurosci* 27: 4799-4809.
- 681 Neher JJ, Emmrich JV, Fricker M, Mander PK, They C, Brown GC (2013) Phagocytosis
682 executes delayed neuronal death after focal brain ischemia. *PNAS* 110: E4098-4107.
- 683 Olinger CP, Adams HP Jr, Brott TG, Biller J, Barsan WG, Toffol GJ, Eberle RW, Marler JR
684 (1990) High-dose intravenous naloxone for the treatment of acute ischemic stroke. *Stroke* 21:
685 721-725.

686 Qin L, Block ML, Liu Y, Bienstock RJ, Pei Z, Zhang W, Wu X, Wilson B, Burka T, Hong JS
687 (2005) Microglial NADPH oxidase is a novel target for femtomolar neuroprotection against
688 oxidative stress. *FASEB J* 19: 550-557.

689 Schroeter M, Zickler P, Denhardt DT, Hartung HP, Jander S (2006) Increased thalamic
690 neurodegeneration following ischaemic cortical stroke in osteopontin-deficient mice. *Brain* 129:
691 1426-1437.

692 Wang Q, Zhou H, Gao H, Chen SH, Chu CH, Wilson B, Hong JS (2012) Naloxone inhibits
693 immune cell function by suppressing superoxide production through a direct interaction with
694 gp91phox subunit of NADPH oxidase. *J Neuroinflammation* 9: 32.

695 Wang X, Zhang Y, Peng Y, Hutchinson MR, Rice KC, Yin H, Watkins LR (2016)
696 Pharmacological characterization of the opioid inactive isomers (+)-naltrexone and (+)-naloxone
697 as antagonists of toll-like receptor 4. *Br J Pharmacol* 173: 856-869.

698 Yang QW, Li JC, Lu FL, Wen AQ, Xiang J, Zhang LL, Huang ZY, Wang JZ (2008) Upregulated
699 expression of toll-like receptor 4 in monocytes correlates with severity of acute cerebral
700 infarction. *J Cereb Blood Flow Metab* 28: 1588-1596.

701 Yrjanheikki J, Tikka T, Keinanen R, Goldsteins G, Chan PH, Koistinaho J (1999) A tetracycline
702 derivative, minocycline, reduces inflammation and protects against focal cerebral ischemia with
703 a wide therapeutic window. *PNAS* 96: 13496-13500.

704

705 **Legends**

706

707 **Figure 1. Chemical structure of (-)-naloxone and (+)-naloxone enantiomers.** K_i of (-)-
708 naloxone for antagonizing opioid receptors is in the 1 nM range whereas (+)-naloxone has a very
709 low affinity for opioid receptors with a K_i of 10 000 nM (Iijima et al., 1978).

710

711 **Figure 2. Time course of microglia/macrophage activation after cortical stroke.**

712 Representative images of immunostaining for all microglia/macrophages (Iba1) and phagocytic
713 microglia/macrophages (CD68) from a: ischemic core, b: peri-infarct area, c: striatum, d:
714 thalamus and e: whole brain sagittal section at 2 (**C, D**), 7 (**E, F**), 14 (**G, H**), 28 (**I, J**), 56 (**K, L**)
715 and 112 (**M, N**) days after 90 min dMCAO in rat. Control images (**A, B**) are from the
716 contralateral hemisphere of the stroke brain. Scale bar is 50 μm (high magnification) and 2000
717 μm (low magnification). **O**: An example image of anti-NeuN immunostaining at post-stroke day
718 2 showing in more detail the regions a-d. **P**: Quantitation of CD68+ cells in the thalamus (d) at
719 different time points showing the accumulation and clearance of phagocytic
720 microglia/macrophages in the ipsilateral thalamus. * $p < 0.05$ indicates statistical difference
721 between the ipsilateral thalamus at different time points; # $p < 0.05$ indicates statistical difference
722 between the ipsilateral and contralateral thalamus in each time point, Mann-Whitney U test after
723 Kruskal-Wallis test; $n=4$ in each group. The data represent mean \pm SEM.

724

725 **Figure 3. Activated microglia in the striatum are lined up along axonal bundles after**

726 **cortical stroke.** Immunostaining of rat striatum at post-stroke day 14 for **A**: phagocytic
727 microglia/macrophages (CD68) and **B**: all microglia/macrophages (Iba1). **C**: Double
728 immunofluorescence staining of rat striatum at post-stroke day 14 for phagocytic

729 microglia/macrophages (CD68; red; **D**) and myelin (MBP; green; **E**) with DAPI (blue; **F**). A-B:
730 Scale bar is 200 μ m. C-F: Scale bar is 50 μ m.

731

732 **Figure 4. Time course of astrocyte activation after cortical stroke.** Representative images of
733 immunostaining for astrocytes (GFAP) from the ischemic core (a), peri-infarct area (b), striatum
734 (c) and thalamus (d) at 2 (**B**), 7 (**C**), 14 (**D**), 28 (**E**), 56 (**F**) and 112 (**G**) days after 90 min
735 dMCAo in sagittal rat brain paraffin sections. Control images (**A**) are from the contralateral
736 hemisphere of the stroke brain. Scale bar is 50 μ m in high magnification images and 2000 μ m in
737 low magnification images. The regions analyzed (a-d) are shown in more detail in Fig. 2O.

738

739 **Figure 5. Post-stroke intranasal administration of naloxone enantiomers promotes**
740 **functional recovery.** **A:** Experimental timeline. Intranasal naloxone (or vehicle) was
741 administered twice daily for 7 days post-stroke. D1-D14: post-stroke days 1-14, B = behavioral
742 assay. **B-C:** Effects of (+)-naloxone (0.32 mg/kg; n=27), vehicle (n=25) and stroke with no
743 treatment (n=13) on body asymmetry (B) and Bederson's neurological score test (C). ** p<0.01,
744 *** p<0.001 indicate post hoc comparison between (+)-naloxone and vehicle groups, and #
745 p<0.05, ## p<0.01, ### p<0.001 indicate post hoc analysis between (+)-naloxone and no
746 treatment groups with Mann-Whitney U test after Kruskal-Wallis test. **D-E:** Effects of different
747 doses of (+)-naloxone 0.0008 mg/kg (n=8), 0.008 mg/kg (n=8), 0.08 mg/kg (n=7) and 0.8 mg/kg
748 (n=8) compared to vehicle (n=11) on day 14 post-stroke on body asymmetry (D) and Bederson's
749 neurological score test (E). * p<0.05 and ** p<0.01 indicate pairwise comparison with vehicle, #
750 p<0.05 and ## p<0.01 indicate pairwise comparison with other (+)-naloxone doses with Mann-
751 Whitney U test after Kruskal-Wallis test. **F-G:** Effects of (+)-naloxone (0.32 mg/kg; n=16),

752 vehicle (n=16) and stroke with no treatment (n=13) on vertical (F) and horizontal (G) activity
753 measured for 24h on day 14. ## p<0.01, Mann-Whitney U test after Kruskal-Wallis test. **H-J**:
754 Effects of (-)-naloxone (0.32 mg/kg; n=7) and vehicle (n=11) on body asymmetry test (H),
755 Bederson's neurological score test (I) and body weight (J). ** p<0.01 and *** p<0.001 indicate
756 comparison with vehicle group with Mann-Whitney U test. **K**: Effects of (+)-naloxone (0.32
757 mg/kg, n=27), vehicle (n=25) and no treatment (n=13) on body weight on days 7 and 14 post-
758 stroke. ** p<0.01, one-way ANOVA, Bonferroni's post hoc test. The data represent mean ±
759 SEM.

760

761 **Figure 6. Post-stroke intranasal (+)-naloxone decreases infarction area and neuronal loss in**
762 **the thalamus. A:** Average infarction size calculated from NeuN negative area at day 14 post-
763 stroke. * p<0.05, Student's *t*-test. **B:** The average number of neurons (NeuN+ cells) in the
764 ipsilateral thalamus at day 14 post-stroke expressed as a percentage of the contralateral thalamus.
765 * p<0.05 and ** p<0.01 indicate pairwise comparison with the control group with Mann-
766 Whitney U test following Kruskal-Wallis test. **C:** Representative photomicrographs of anti-NeuN
767 immunostained brain sections with infarction area delineated. **D-F:** Representative
768 photomicrographs of anti-NeuN immunostaining of ipsilateral thalamus in naïve (D), control (E)
769 and (+)-naloxone (F) treated rats. Scale bar is 150 µm. naïve = no stroked rats (n=6), control =
770 stroke rats with vehicle or no treatment (n=18), (+)-naloxone (0.32-0.8 mg/kg; n=10). The data
771 represent mean ± SEM.

772

773 **Figure 7. Post-stroke intranasal (+)-naloxone decreases microglia/macrophage activation in**
774 **the striatum and thalamus. A-B:** Microglia/macrophages (Iba1+ cells) were counted with

775 unbiased stereology in the ipsilateral (A) and contralateral (B) striatum. * $p < 0.05$, ** $p < 0.01$
776 indicate pairwise comparison with the control group with Bonferroni's post hoc test following
777 one-way ANOVA. **C:** The area of Iba1+ cells in the ipsilateral thalamus expressed as a
778 percentage of the contralateral thalamus. * $p < 0.05$, *** $p < 0.001$ indicate pairwise comparison
779 with the control group; ## $p < 0.01$ indicates comparison with the naïve group with Mann-
780 Whitney U test following Kruskal-Wallis test. **D-K:** Representative photomicrographs of anti-
781 Iba1 immunostaining of ipsilateral striatum (D-E) and thalamus (F-G) in control (D, F) and (+)-
782 naloxone (E, G) treated rats; H-K show high magnification. Black arrow shows a typical Iba1+
783 cell. Scale bar is 1000 μm (D-G) and 50 μm (H-K). naïve = no stroked rats ($n=6$), control =
784 stroke rats with vehicle or no treatment ($n=18$), (+)-naloxone (0.32-0.8 mg/kg; $n=10$). The data
785 represent mean \pm SEM.

786

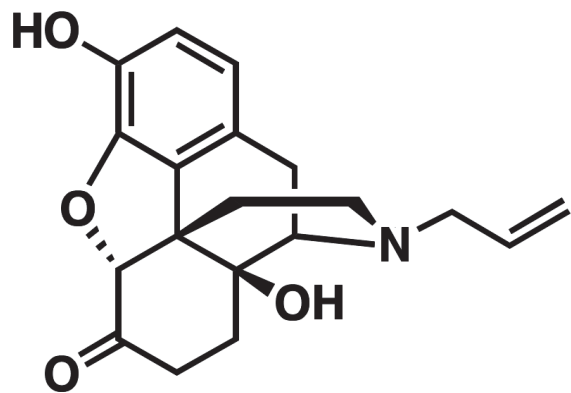
787 **Figure 8. The effect of different pre- and post-stroke treatment with (+)-naloxone on**
788 **infarct volume and functional recovery.** **A:** Experimental timeline. Intranasal (+)-naloxone or
789 vehicle was administered three times: 12h and 1h before dMCAo and immediately after
790 reperfusion. Infarction volume was determined by 2,3,5-triphenyltetrazolium chloride (TTC)
791 staining 2 days after stroke. **B:** Average infarction volume (mm^3) on day 2 post-stroke in vehicle
792 ($n=7$) and (+)-naloxone (0.32 mg/kg; $n=8$) pre-treated rats. Pre-stroke intranasal administration
793 of (+)-naloxone was not neuroprotective in 60 min dMCAo. **C:** Experimental timeline. (+)-
794 Naloxone was delivered intranasally twice daily for 7 days post-stroke starting from post-stroke
795 day 3. **D:** The effect of (+)-naloxone (0.8 mg/kg; $n=6$) and vehicle ($n=7$) treatment from post-
796 stroke day 3 to post-stroke day 10 on body asymmetry test. **E:** Experimental timeline. (+)-
797 Naloxone was delivered into the ventricle via mini-osmotic pumps for 12 days post-stroke

798 starting from post-stroke day 2. **F:** The effects of 12 day continuous delivery of (+)-naloxone
799 (1.15 mg/24h; n=7) and vehicle (n=8) on body asymmetry test and **G:** body weight. In A, C and
800 E: D = the indicated post-stroke day, B = behavioral assay. The data represent mean \pm SEM.

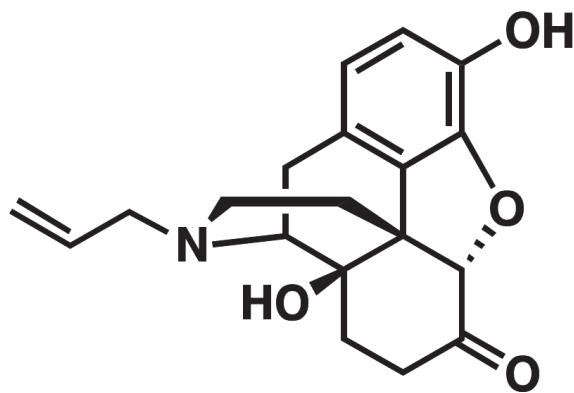
801

802 **Figure 9. Naloxone reduced TNF- α secretion from CD11b+ cells. A:** LPS induced TNF- α
803 secretion from CD11b-expressing cells isolated from the infarct area of rat brain 7 days after
804 dMCAo. ** p<0.01, Mann-Whitney U test; control n=6, LPS n=5 in 2 independent experiments.

805 **B:** CD11b+ cells were isolated from the infarct area and treated with different concentrations of
806 naloxone as indicated for 20h. *p<0.05; **p<0.01 indicate pairwise comparison with the control
807 group by Dunnett's post hoc test following one-way ANOVA; control n=9, naloxone n=8-9 in 3
808 independent experiments. The culture medium was analyzed using TNF- α ELISA. The data
809 represent mean \pm SEM.



(-)-Naloxone



(+)-Naloxone

